

# Cobalt Additives Influence on Phase Composition and Defect Structure of Manganese Dioxide Prepared from Fluorine Containing Electrolytes

G.V. SOKOLSKY<sup>a,\*</sup>, S.V. IVANOV<sup>a</sup>, N.D. IVANOVA<sup>b</sup>, YE.I. BOLDUREV<sup>b</sup>,  
O.V. KOBULINSKAYA<sup>a</sup> AND M.V. DEMCHENKO<sup>a</sup>

<sup>a</sup>National Aviation University, Cosmonaut Komarov Av. 1, 04058 Kiev 58, Ukraine

<sup>b</sup>Institute of General and Inorganic Chemistry of Ukrainian National Academy of Science  
Palladin Av. 32-34, 252680 Kiev 142, Ukraine

Manganese dioxide samples were prepared from fluorine containing electrolytes with additives of  $\text{Co}^{2+}$  ions. Atomic absorption spectroscopy, thermogravimetric analysis, X-ray diffraction, scanning electron microscopy with energy dispersive X-ray analysis were the methods of the samples characterisation. Manganese dioxide at the presence of cobalt forms nanosized ramsdellite structure crystallites of mostly needle-like morphology with significant content of hydroxide groups. The main phase state in manganese dioxide samples obtained at the presence of cobalt is  $\gamma\text{-MnO}_2$  with ramsdellite structure and low content of intergrowth defects. The sample doped both with lithium and cobalt can be indexed to a hollandite-type structure (tetragonal; space group  $I4/m$ ) of  $\alpha\text{-MnO}_2$ .

PACS numbers: 61.66.Fn, 61.72.-y, 85.40.Ry

## 1. Introduction

Oxide materials are of considerable importance in various practical applications. Recent achievements in the field of batteries have given impetus to investigations of 3d-series transition metal oxides [1]. These oxide systems attract also attention from the point of view of their structural complexity. They can vary composition, structure ordering, and properties in broad limits [2]. Almost all of the research and commercialisation of cathode materials of Li batteries has centred on the layered oxides, spinels, and more open structures of transition metal oxides, like many of the vanadium oxides, the tunnel compounds of manganese dioxide etc. [1, 3, 4]. The development of the direct methanol fuel cell (DMFC) has grown significantly over the past decade. Manganese dioxide is shown to be a relatively cheap and promising alternative to noble metals electrode materials in DMFC [5]. It is also an active catalyst of oxidation of many other organic compounds [6, 7].

Manganese dioxide forms a variety of polymorphs with hexagonal, tunnel, layered, and spinel structures. The crystals of tunnelled polymorphs consists of  $n \times m$  edge-shared  $\text{MnO}_6$  octahedral chains, which are corner-

-connected to form one-dimensional channels. They are usually named manganese oxide octahedral molecular sieves (OMS) [6]. Among these compounds, tunnel structures with regular lattice such as pyrolusite ( $1 \times 1$ ,  $\beta\text{-MnO}_2$ ), ramsdellite ( $1 \times 2$ ,  $\gamma\text{-MnO}_2$ ), hollandite ( $2 \times 2$ ,  $\alpha\text{-MnO}_2$ ),  $2 \times 3$  romanechite and  $3 \times 3$  todorokite can be distinguished. Electrochemically active form of  $\text{MnO}_2$  in Leclanche and alkaline primary batteries is  $\gamma\text{-MnO}_2$ .  $\varepsilon\text{-MnO}_2$  is a polymorph with hexagonal symmetry, which has similar to  $\gamma\text{-MnO}_2$  electrochemical activity [8]. The latter forms, referring to their most frequently used method of formation (electrodeposition from very acidic  $\text{MnSO}_4$  solutions) are known also as electrolytic manganese dioxide (EMD).

The electrochemical, catalytic, and electrocatalytic properties of manganese dioxide materials is shown to vary depending upon their defects nature and, in turn, their concentration [9, 10]. The nonstoichiometry of manganese dioxide is defined by ions of manganese of mixed valence that occupy the same sites of crystal lattice [9], cation vacancies [10, 11], and defects of intergrowth (De Wolff defects) [12].

Our recent researches have revealed that electron paramagnetic resonance (EPR) data can be the measure of defects concentration, which are responsible for electrochemical activity of manganese dioxide samples. The partial substitution of  $\text{Mn}^{4+}$  ions for  $\text{Mn}^{3+}$  modifies the character of the exchange interaction and causes

\* corresponding author; e-mail:  
gvsokol@rambler.ru, sokol@bg.net.ua

the broadening of the recorded signal. The good correlation of EPR signal width,  $\Delta B$ , in different samples and the  $\text{Mn}^{3+}/\text{Mn}^{4+}$  ratio as well as the specific capacity of  $\text{MnO}_2$ -Zn alkaline coin elements have been established [13].

The up to date publications introduce controversial viewpoints on the nature of structural defects and interpretation of X-ray diffraction (XRD) patterns of EMDs. On the one hand, it is a group of compounds that derive from that of ramsdellite by introducing structural defects of intergrowth (i.e. faults of pyrolusite in ramsdellite) and microtwinning [14–16]. On the other hand, multi-phase model of EMDs was proposed in [17]; the presence of  $\varepsilon$ - $\text{MnO}_2$  as a major component of EMD has been demonstrated in [18].

The usual methods of characterisation and study of manganese dioxide by powder XRD cannot be followed. From this point of view, the International Common Samples (ICS) of manganese dioxide have been introduced in line with the leading world producers of this material and a comparison with the set of ICS reference XRD-patterns is frequently used [19].

Electrodeposition is known to be a prospective method of nanopowders and nanofilms preparation. Fluorine containing electrolytes allow fast producing electrolysis products with high defect concentration [20] including manganese dioxide preparation [21]. The addition of dopants can be other instrument of adjustment of phase composition, defects nature and concentration in nanostructured samples. Combined with electrodeposition, doping technique showed interesting results. Additives of lithium during electrosynthesis increase electrochemical activity in aqueous alkaline batteries and the content of opened structure polymorphs of manganese dioxide [22]. For instance, the presence of new member of the tunnelled polymorphs family with large size tunnels formed by  $\text{MnO}_6$  octahedrons ( $2 \times 4$ ) of general formula  $\text{Li}_{16}\text{Mn}_{24}\text{O}_{48}$  was detected by a transmission electron microscopy (TEM) study. It was suggested that this structure could be stable even at lower content of lithium in the formula. We suppose that such materials are promising catalysts of organic compounds oxidation, and electrode materials for power sources including lithium ion batteries [23].

The aim of this paper is to study the influence of cobalt additives on the structure defects, phase and chemical compositions of manganese dioxide electrodeposited from the fluorine containing electrolytes.

## 2. Experimental

The products of anode oxidation of manganese(II) ions at the presence of additives of cobalt ions were synthesized from fluorine containing electrolytes [21]. The concentration ranges for dopants used in the electrolyte were chosen on the basis of the solubility of the corresponding compounds and some preliminary results of chemical analysis.

The electrodeposition of the doped manganese dioxide was studied on a Pt anode in 0.2 M HF containing 0.7 M  $\text{MnSO}_4$ . For doping with cations, the corresponding salts were introduced by the addition of solutions of 0.001–0.1 mol  $\text{l}^{-1}$   $\text{CoSO}_4$ . A constant current density range was 1–6 A  $\text{dm}^{-2}$  at room temperature. A plate of steel of 1CH18N10 T grade served as a cathode. The precipitated deposit was decanted filtered off through filter Shotta, rinsed with distilled water, and dried in air at 80–90 °C for 1 h.

Some samples were prepared using ternary electrolytes by ions of metals [24]. They contained, besides manganese sulfate and hydrofluoric acid HF, additives of cobalt sulfate and lithium hydroxide. The dopant ions were introduced by the addition of 0.03–1 mol  $\text{l}^{-1}$  of  $\text{CoSO}_4$  and 0.1–4 mol  $\text{l}^{-1}$  LiOH. For the purpose of comparison there were analysed XRD-patterns and some other data of the sample doped by lithium and cobalt (0.05 mol  $\text{l}^{-1}$  of  $\text{CoSO}_4$ , 0.15 mol  $\text{l}^{-1}$  LiOH), ICS #10, Kerr-McGee Corp. (USA) [19], the serial sample of EMD-2 grade manganese dioxide (OST-6-22-34-76) produced by electrolysis of sulfate electrolyte, Republic of Georgia.

The content of manganese, cobalt, and lithium in the doped samples was determined by atomic absorption spectroscopy (AAS). XRD analyses of the products were carried out on a DRON-3 X-ray diffractometer with  $\text{CuK}_\alpha$  radiation ( $\lambda = 0.154184$  nm) or  $\text{MoK}_\alpha$  ( $\lambda = 0.070930$  nm). Scanning electron microscope images were obtained at 3.00 kV with a Carl Zeiss ULTRA PLUS 40-24 II electron microscope. Thermogravimetric analysis (TGA) data were collected with a derivatograph of Paulic-Paulic-Erdey (Hungary). The temperature was increased from ambient to 900 °C at a rate of 10 °C/min.

## 3. Results and analysis

Disordered and semi-amorphous oxides of manganese have been prepared by the anode electrodeposition from fluoride containing electrolytes of manganese sulfate at the presence/absence of additives of cobalt(II) (cobalt(II) and lithium). Our choice of fluorine containing electrolytes was by no means accidental. As mentioned above, one can control the composition and properties of oxide compounds and produce them at high rates. Fluoride containing complexes in electrolytes of manganese have higher mobility at electrodeposition of manganese dioxide. For instance, it was found [25] that particles  $[\text{Mn}(\text{H}_2\text{O})_6(\text{SO}_4)_2(\text{NH}_4)\text{F}]^{2-}$  are responsible for high mobility of manganese in these electrolytes at the presence of  $\text{NH}_4^+$ . Fluoride ions increase markedly the content of incorporated cobalt at anode deposition of lead dioxide. The authors [26] supposed also that formation of F-containing complexes, probably bearing a partial negative charge, such as  $[\text{Co}(\text{OH})_x\text{F}_y]^{(2-x-y)}$ , is responsible for the increase of Co surface concentration due to more favourable adsorption.

The maximal content of incorporated cobalt in our experiments made up about 3% at minimal concentration of

manganese ions in ternary electrolytes [24]. Such samples were X-ray amorphous and it was shown with the help of TEM study that at the presence of additives the needle-like crystallites lost their crystallinity. In this work, the dependence of cobalt content in electrodeposited samples upon the composition of manganese and cobalt in electrolyte is summarised in Table I. Our results of chemical analysis agree well with data of electrodeposition of manganese dioxide at the presence of cobalt obtained by the electrochemical-hydrothermal route from sulfate electrolytes [27]. The maximal content of cobalt 3% for materials synthesised at  $\text{pH} \geq 4$  is in agreement with our data [24].

TABLE I

Composition of anode manganese dioxide deposits obtained at the presence of additives of cobalt.

Sample	Cobalt concentration in electrolyte	Mn [%]	Co [%]
1	0.001 M $\text{CoSO}_4$	54.1	0.007
2	0.01 M $\text{CoSO}_4$	42.0	0.012
3	0.1 M $\text{CoSO}_4$	34.6	0.183
4	–	51.0	–

Thermogravimetric investigations were performed to check the content of hydroxide groups and physically sorbed water. Hydroxide groups stabilise redox pairs  $\text{Mn}^{4+}/\text{Mn}^{3+}$  (“Coleman” protons [10]), build up cation vacancies (“Ruetschi” protons [11, 28]) and some other defects. The typical derivatogram of manganese dioxide samples doped by cobalt is demonstrated in Fig. 1.

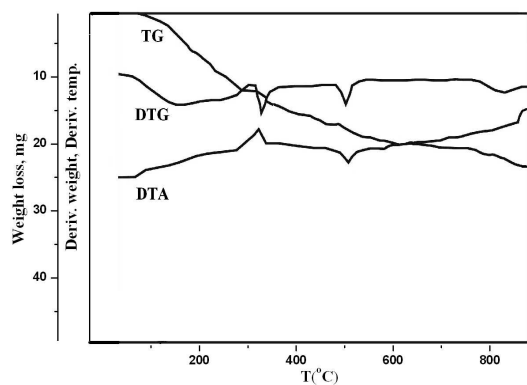


Fig. 1. Derivatogram of manganese dioxide sample 1 doped by cobalt.

The exoeffect of DTA curve at  $340^\circ\text{C}$  and endoeffect at  $500^\circ\text{C}$  characterise a phase transition to more thermodynamically stable pyrolusite polymorph of manganese dioxide and its decomposition to  $\text{Mn}_2\text{O}_3$ , respectively [29]. Our EMDs have an initial weight loss of physically sorbed water near  $100^\circ\text{C}$ . The second loss takes place near  $340^\circ\text{C}$  from the loss of vacancies and lattice protons and formation of the so-called heat treated manganese dioxide (HEMD) with defect pyrolusite structure.

The last effect is the loss of oxygen near  $500^\circ\text{C}$  [16]. A comparative analysis of the weight loss in Table II indicates that the addition of cobalt(II) ions increases markedly the content of physically sorbed water. The latter influences the tendency of manganese, hydroxide group content and oxygen loss change in samples. The weight loss of OH groups is practically identical in both cases (8.5 and 8.3, respectively) without physically sorbed water. Their significant content can be attributed to the presence of  $\text{Mn}^{3+}$  and cationic vacancies in structure. The low weight loss at  $\text{MnO}_2$  to  $\text{Mn}_2\text{O}_3$  transition confirms this suggestion indirectly (electrochemically synthesised samples of manganese dioxide usually have the weight loss in this temperature range about 4–5%).

TABLE II

Results of a thermogravimetric study of samples 1 and 3.

Effects	Weight loss [%]	
	sample 1	sample 3
$\text{H}_2\text{O}$	6.1	15.6
OH	1.4	1.2
(surface, $150\text{--}200^\circ\text{C}$ [29])		
OH	6.6	5.8
(bulk, $200\text{--}400^\circ\text{C}$ [29])		
total OH group content	$\approx 8$	$\approx 7$
oxygen loss	1.9	1.4
	( $400\text{--}513^\circ\text{C}$ )	( $400\text{--}490^\circ\text{C}$ )

Figure 2 shows the powder XRD pattern of samples 2–4 (curves 3–5). Curves 1–2 represent electrolytic  $\gamma\text{-MnO}_2$  (EMD ICS #10, Kerr-McGee Corp.), serial sample of EMD-2 grade (Republic of Georgia), respectively. For the purpose of comparison the sample doped with lithium and cobalt obtained from fluorine containing electrolytes (curve 6) is also shown in Fig. 2. The XRD pattern of the latter sample is quite similar to that of  $\alpha\text{-MnO}_2$ . All strong diffraction peaks of this sample can be indexed to a hollandite-type structure (tetragonal; space group  $I4/m$ ) [30]. This result agrees well with X-ray diffraction characterisation of  $\alpha\text{-MnO}_2$  and its metal-doped  $\text{K}_y(\text{Mn}_{0.88}\text{M}_{0.12})\text{O}_2$  ( $y = 0.08\text{--}0.12$ ;  $\text{M} = \text{Co}$  or  $\text{Fe}$ ), synthesised from aqueous solutions consisting of 1 M  $\text{MnSO}_4$  and 1 M  $\text{MSO}_4$  ( $\text{M} = \text{Co}, \text{Fe}$ ) followed by their further oxidation by  $\text{K}_2\text{S}_2\text{O}_8$  at  $80^\circ\text{C}$  [31].

It can be seen in Fig. 2 that the main phase state of manganese dioxide samples 2,3 at the presence of cobalt is  $\gamma\text{-MnO}_2$  with ramsdellite structure and poor crystallinity (see also [24]) unlike samples doped with lithium [32] or cobalt and lithium in Fig. 2 (curve 6). The decrease of relative intensity of  $\gamma\text{-MnO}_2$  (211) and (221) reflections at  $d \approx 0.213$  nm and 0.164 nm, respectively, is a common feature of manganese dioxide samples 3–5 obtained from fluorine containing electrolytes.

The appearance of a very broad reflection (110) of  $\gamma\text{-MnO}_2$  can be explained from the point of view of

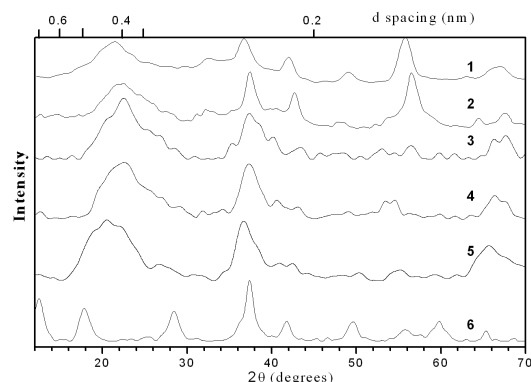


Fig. 2. XRD patterns of manganese dioxide samples: samples 2–4 (curves 3–5, respectively), doped by lithium and cobalt EMD (curve 6), EMD Kerr-McGee Corp. (curve 1), EMD-2, Republic of Georgia (curve 2).

microtwinning and a random intergrowth of manganese dioxide polymorphs ramsdellite and pyrolusite [14]. The shift of this peak to lower  $d$  (to 110 reflection of pyrolusite) allows the analysis of the relative number of pyrolusite intergrowth defects in samples doped by cobalt. Chabre and Pannetier calculated the XRD patterns of  $\text{MnO}_2$  structures ranging from pure ramsdellite as the function of increasing De Wolff defects to the limiting case of perfect pyrolusite [14]. The semiquantitative comparison between XRD-patterns of our samples doped by cobalt and calculated results [14] showed that the samples have low content of pyrolusite fraction (smaller than about 5–10%).

The position of (110) reflection of sample 1 obtained without additives is shifted to higher  $d$  ( $\approx 0.43$ – $0.44$  nm) in comparison with XRD-patterns of EMD (Fig. 2, curves 1, 2), ramsdellite (JCPDS 82-2169, 72-1983) and samples doped by cobalt. In our opinion, this fact points out the intergrowth of more opened polymorph hollandite to ramsdellite oxide matrix due to the shift of (110) ramsdellite reflection to the direction of (110) reflection of hollandite at  $d \approx 0.69$  nm (Fig. 2 (curve 6)); similarly ramsdellite/pyrolusite intergrowth. This suggestion is in agreement with our unpublished results of micropore analysis by Horvath–Kawazoe method ( $2 \times 2$  tunnels that have pore size 0.53 nm were detected in sample 1 as well as in samples that contain  $\alpha$ - $\text{MnO}_2$ ). Experimental TEM, convergent beam electron diffraction data in [33] revealed “interconnection” of  $\alpha$ - $\text{MnO}_2$  and ramsdellite- $\text{MnO}_2$  grains which exhibit mutual crystallographic orientation. Further researches aimed at finding an explanation of  $2 \times 2$  tunnels appearance in undoped sample without strong  $\alpha$ - $\text{MnO}_2$ (110) reflection (Fig. 2) are necessary.

Although the influence of cobalt(II) on the structure of electrodeposited manganese dioxide is evident, the direct observations of localisation of cobalt were not successive. The scanning electron microscopy investigations combined with energy dispersive analysis could not show

us the presence of cobalt at the surface layer. The needle-like and plate-like nanosized crystallites that both belong to manganese dioxide have been detected. The content of plate-like crystallites is low. The SEM image in Fig. 3 illustrates needle-like nanocrystallites of sample 1.

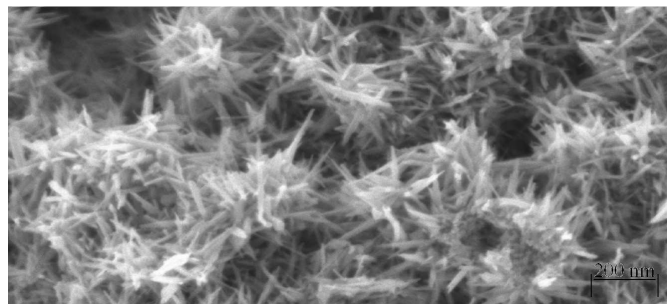


Fig. 3. SEM image of electrolytic manganese dioxide doped by cobalt.

Cobalt ions have the low tendency to oxidation at the presence of manganese(II) in an electrolyte.  $\text{Co}^{2+}$  can be adsorbed at the interface electrode/electrolyte and occupy the sites of manganese(II) or cationic vacancies. The similar behaviour of ions of cobalt(II) during electrodeposition of lead dioxide was described by Velichenko et al. [26]. At heavy doping by cobalt (about 3%) all manganese dioxide samples synthesised in our laboratory were X-ray amorphous and needle-like crystallites lost their initial perfect shape [24].

On the other hand,  $\alpha$ - $\text{MnO}_2$  polymorph formation at the presence of lithium and low doping by cobalt (Fig. 2 (curve 6)) indicates that lithium could simultaneously occupy structure channels  $2 \times 2$  stabilising hollandite structure type. The large channels of hollandite structure type are not empty. They usually contain water or cations of metals [33]. Therefore, undoped manganese dioxide with ramsdellite structure needs additives of alkaline metals to completely realise  $\alpha$ - $\text{MnO}_2$  phase state. Finally, at low doping the presence of cobalt decreases intergrowth of both pyrolusite (smaller than 5–10%) and  $\alpha$ - $\text{MnO}_2$ .

#### 4. Summary

Manganese dioxide samples were prepared from fluorine containing electrolytes with additives of cobalt(II) ions. They form nanosized crystallites of mostly needle-like morphology with a significant content of hydroxide groups that stabilise predominantly  $\text{Mn}^{3+}$  defects, cationic vacancies, and the defects of intergrowth.

The main phase state in manganese dioxide samples obtained at the presence of cobalt is  $\gamma$ - $\text{MnO}_2$  with ramsdellite structure and low content of intergrowth defects. The sample doped both with lithium and cobalt can be indexed to a hollandite-type structure (tetragonal; space group  $I4/m$ ) of  $\alpha$ - $\text{MnO}_2$ . It indicates that lithium can occupy structure channels  $2 \times 2$  stabilising

hollandite structure type. Probably, the electrodeposited manganese dioxide obtained without additives from fluoride containing electrolytes contains defects of intergrowth of more opened hollandite tunnelled polymorph and the presence of alkaline metals is necessary to support  $\alpha$ -MnO<sub>2</sub> phase state.

### Acknowledgments

The authors would like to thank the Ministry of Education and Science and National Aviation University in Ukraine for the financial support within grant No. 0108U004063.

### References

- [1] M.S. Whittingham, *Chem. Rev.* **104**, 4271 (2004).
- [2] P. Kofstad, *Oxidat. Metals* **44**, 3 (1995).
- [3] A. Le, Gal La Salle, A. Verbaere, Y. Piffard, D. Guyomard, in: *NATO Science Series*, Vol. 85, Ed. C. Julien, Z.B. Stoinov, Kluwer Academic Publishers, Dordrecht 2000, p. 241.
- [4] Y. Song, P.Y. Zavalij, M.S. Whittingham, *J. Electrochem. Soc.* **152**, A762 (2005).
- [5] J.S. Rebello, P.V. Samant, J.L. Figueredo, J.B. Fernandes, *J. Power Sources* **153**, 36 (2006).
- [6] S.L. Suib, *Chem. Innovation* **30**, 27 (2000).
- [7] V.D. Makwana, L.J. Garces, J. Liu, J. Cai, Y.-C. Son, S.L. Suib, *Catalysis Today* **85**, 225 (2003).
- [8] P.M. De Wolff, J.W. Visser, R. Giovanoli, R. Brutsch, *Chimia* **32**, 257 (1978).
- [9] J. Brenet, *J. Power Sources* **4**, 183 (1979).
- [10] P. Ruetschi, R. Giovanoli, *J. Electrochem. Soc.* **135**, 2663 (1988).
- [11] H. Abbas, S.A. Nasser, *J. Power Sources* **58**, 15 (1996).
- [12] P.M. de Wolff, *Acta Crystallogr.* **12**, 341 (1959).
- [13] M. Kakazey, N. Ivanova, Y. Boldurev, S. Ivanova, G. Sokolsky, J.G. Gonzalez Rodriguez, M. Vlasova, *J. Power Sources* **114**, 170 (2003).
- [14] Y. Chabre, J. Pannetier, *Prog. Solid State Chem.* **23**, 1 (1995).
- [15] L.I. Hill, A. Verbaere, *J. Solid State Chem.* **177**, 4706 (2004).
- [16] W. Bowden, T. Bofinger, F. Zhang, N. Iltchev, R. Sirotna, Y. Paik, H. Chen, C. Grey, S. Hackney, *J. Power Sources* **165**, 609 (2007).
- [17] A.H. Heuer, A.Q. He, P.J. Hughes, F.H. Feddrix, *ITE Lett.* **1**, B50 (2000).
- [18] C.-H. Kim, Z. Akase, L. Zhang, A.H. Heuer, A.E. Newman, P.J. Hughes, *J. Solid State Chem.* **179**, 753 (2006).
- [19] D.G. Malpas, F.L. Tye, in: *Handbook of Manganese Dioxides Battery Grade*, Eds. D. Glover, B. Schumm Jr., A. Kozawa, IBA Inc & JEC Press Inc., Brunswick 1989, Ch. IV.
- [20] N.D. Ivanova, S.V. Ivanov, *Russian Chem. Rev.* **62**, 907 (1993).
- [21] N. Ivanova, Y. Boldurev, G. Sokolsky, I. Makeeva, *Russ. J. Appl. Chem.* **75**, 1420 (2002).
- [22] G. Sokolsky, N. Ivanova, S. Ivanov, Ye. Boldyrev, in: *5th Spring Annual Meeting of the ISE, Dublin (Ireland)*, 2007, Book of Abstracts, p. 153.
- [23] G. Sokolsky, N. Ivanova, Y. Boldurev, S. Ivanov, *XVII Ukrainian Inorganic Chem. Conf. Proc., Lviv*, 2008, p. 160.
- [24] G. Sokolsky, N. Ivanova, S. Ivanov, T. Tomila, Ye. Boldyrev, *Sci. Sintering* **39**, 273 (2007).
- [25] I.S. Makeeva, N.D. Ivanova, V.V. Trachevsky, *Ukr. Khim. Zh.* **66**, 88 (2000).
- [26] A.B. Velichenko, R. Amadelli, G.L. Zucchini, D.V. Girenko, F.I. Danilov, *Electrochim. Acta* **45**, 4341 (2000).
- [27] E. Machevaux, L.I. Hill, A. Verbaere, D. Guyomard, in: *New Trends in Intercalation Compounds for Energy Storage and Conversion*, Eds. K. Zaghib, C.M. Juilien, J. Prakash, Electrochemical Social Proceedings, Vol. PV 2003-20, Pennington 2003, p. 461.
- [28] C. Pitteloud, M. Nagao, K. Itoh, R. Kanno, *J. Solid State Chem.* **181**, 467 (2008).
- [29] K.M. Parida, S.B. Kanungo, *Thermochim. Acta* **66**, 275 (1983).
- [30] N. Kijima, T. Ikeda, K. Oikawa, F. Izumi, Y. Yoshimura, *J. Solid State Chem.* **177**, 1258 (2004).
- [31] N. Kumagai, T. Sasaki, S. Oshitari, S. Komaba, *J. New Mater. Electrochem. Systems* **9**, 175 (2006).
- [32] G. Sokolsky, S. Ivanov, N. Ivanova, Y. Boldurev, *Powder Metall. Met. Ceram.* **45**, 158 (2006).
- [33] C.S. Johnson, M.F. Mansuetto, M.M. Thackeray, Y. Shao-Horn, S.A. Hackney, *J. Electrochem. Soc.* **144**, 2279 (1997).